Chapter 18

Isotopically Nonstationary ^{13}C Metabolic Flux Analysis

Lara J. Jazmin and Jamey D. Young

Abstract

^{13}C metabolic flux analysis (MFA) is a powerful approach for quantifying cell physiology based upon a combination of extracellular flux measurements and intracellular isotope labeling measurements. In this chapter, we present the method of isotopically nonstationary ^{13}C MFA (INST-MFA), which is applicable to systems that are at metabolic steady state, but are sampled during the transient period prior to achieving isotopic steady state following the introduction of a ^{13}C tracer. We describe protocols for performing the necessary isotope labeling experiments, for quenching and extraction of intracellular metabolites, for mass spectrometry (MS) analysis of metabolite labeling, and for computational flux estimation using INST-MFA. By combining several recently developed experimental and computational techniques, INST-MFA provides an important new platform for mapping carbon fluxes that is especially applicable to animal cell cultures, autotrophic organisms, industrial bioprocesses, high-throughput experiments, and other systems that are not amenable to steady-state ^{13}C MFA experiments.

Key words: Metabolic flux analysis, Isotopically nonstationary, Isotopomer analysis, Mass spectrometry, Elementary metabolite unit, Isotopomer modeling

1. Introduction

The ability to quantitatively map intracellular carbon fluxes using isotope tracers and metabolic flux analysis (MFA) is critical for identifying pathway bottlenecks and elucidating network regulation in biological systems, especially those that have been engineered to alter their native metabolic capacities (1, 2). Typically, MFA relies on the assumption of both metabolic and isotopic steady state. Achieving this situation experimentally involves (1) equilibrating the system in a stable metabolic state, (2) introducing an isotopically labeled substrate without perturbing the metabolic steady state, (3) allowing the system to establish a new isotopic steady state that is dictated by the underlying metabolic fluxes, and (4) measuring isotopic labeling in the fully equilibrated system

Hal S. Alper (ed.), *Systems Metabolic Engineering: Methods and Protocols*, Methods in Molecular Biology, vol. 985,
DOI 10.1007/978-1-62703-299-5_18,

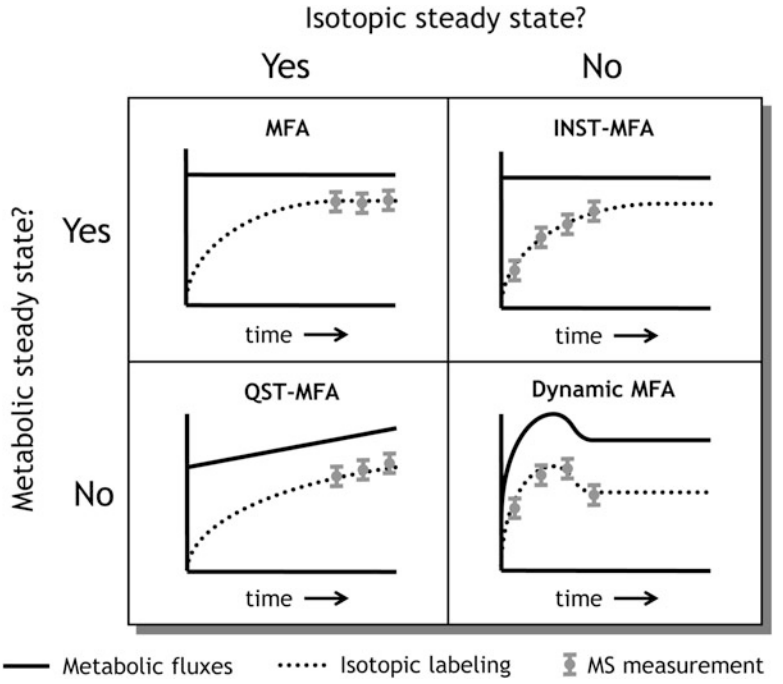

Fig. 1. Overview of different MFA methodologies. The relative speed of metabolic and isotopic dynamics will influence the type of MFA study performed. The *upper-left panel* shows the typical MFA setup under both metabolic and isotopic steady state. The *upper-right panel* shows INST-MFA at metabolic steady state, but not isotopic steady state. The *bottom-left panel* shows quasi-stationary MFA (QST-MFA) at isotopic quasi-steady state, but not metabolic steady state. The *bottom-right panel* shows Dynamic MFA, which is at neither metabolic nor isotopic steady state.

(Fig. 1, upper-left panel). Depending on the relative speed of metabolic versus isotopic dynamics, however, other experimental scenarios can be envisioned. If the isotopic labeling responds quickly to metabolic perturbations, quasi-stationary MFA (QST-MFA; Fig. 1, lower-left panel) can be applied to obtain a series of instantaneous snapshots that describes the variation in metabolic fluxes over time (3, 4). Because of the quasi-steady-state assumption on isotopic labeling, the isotopomer balances remain algebraic in nature, and the computational treatment applied to each time slice is essentially identical to that of steady-state MFA. Conversely, if labeling occurs slowly but metabolism is maintained in a fixed state, isotopically nonstationary MFA (INST-MFA; Fig. 1, upper-right panel) can be applied to determine fluxes from transient isotope labeling measurements (5). This requires repeated solution of differential balance equations that describe the time-dependent labeling of intermediate metabolites, while iteratively adjusting the flux parameters in those equations to match the experimental measurements. Finally, when measurements are obtained under both metabolically and isotopically nonstationary conditions, a fully

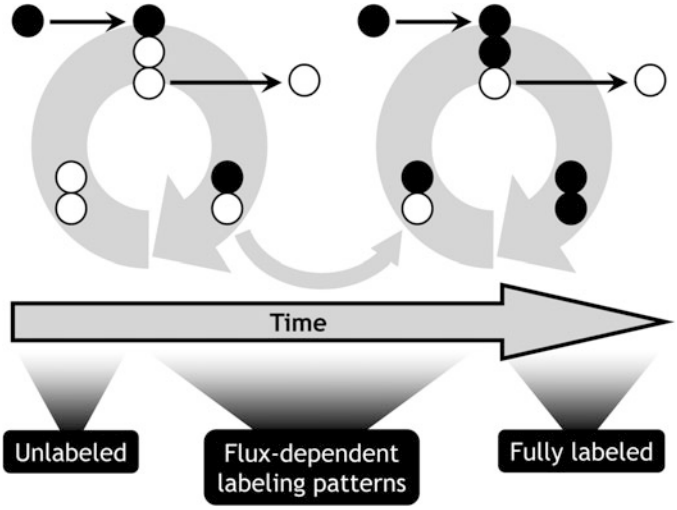

Fig. 2. Example of carbon labeling in an autotrophic system. Following the introduction of a labeled tracer to the system, intracellular metabolites become gradually labeled over time. Once steady-state labeling is achieved, all metabolites are uniformly ^{13}C labeled irrespective of fluxes and intracellular pool sizes. Labeling patterns observed during the isotopically transient period, however, can be computationally analyzed to determine fluxes.

dynamic modeling approach is required to estimate time-dependent fluxes (Fig. 1, lower right). This scenario has been referred to as Dynamic MFA (6–8), and it is an area of ongoing research for which appropriate methodologies and software tools are currently under development.

In this chapter, we present up-to-date protocols for performing INST-MFA under conditions of metabolic steady state, which has now matured to the point where optimized methodologies and software tools are rapidly emerging. INST-MFA holds a number of unique advantages over approaches that rely solely upon steady or quasi-steady isotopomer measurements.

1. ^{13}C INST-MFA can be applied to estimate fluxes in autotrophic or methylotrophic systems, which consume only single-carbon substrates (9, 10). This task is impossible with stationary ^{13}C MFA due to the fact that all carbon atoms in the system are derived from the same source and therefore will become uniformly labeled at steady state regardless of the flux distribution (Fig. 2). However, the transient labeling patterns that emerge following a step change from unlabeled to ^{13}C-labeled substrates can be analyzed by INST-MFA to determine fluxes with precision.

2. INST-MFA is ideally suited to systems that label slowly due to the presence of large intermediate pools or pathway bottlenecks. This approach not only avoids the additional time and cost of feeding isotope tracers over extended periods (e.g., see Zhao et al. (11)) but may become absolutely necessary in cases where the system cannot be held in a fixed metabolic state long enough to allow isotopic labeling to fully equilibrate. As a result, INST-MFA is expected to become an indispensible tool for extending MFA approaches to studies of mammalian systems (12–14), industrial bioprocesses (5, 15), and other scenarios where attaining a strict isotopic steady state may be impractical.
3. INST-MFA provides increased measurement sensitivity to system parameters. A prime example is the observation that nonstationary labeling measurements are sensitive to metabolite pool sizes, whereas steady-state measurements are not (16, 17). This enables INST-MFA to estimate not only fluxes but intracellular metabolite concentrations as well, which represents a potential framework for integrating metabolomic analysis with MFA. Several studies have also noted that nonstationary measurements often exhibit increased sensitivity to fluxes, especially to certain exchange fluxes (16, 18). Therefore, collecting transient isotopic measurements over a range of time points can improve the precision of flux estimates through application of INST-MFA.

Despite its advantages, the increased complexity of INST-MFA introduces additional difficulties at both the computational and experimental levels. However, these challenges have been largely addressed through recent technical advances.

1. The solution of large-scale ordinary differential equation (ODE) models poses a substantial challenge to efficiently simulating transient isotope labeling experiments. The application of EMU decomposition to INST-MFA has greatly reduced this computational burden and has enabled determination of fluxes and accurate confidence intervals in biologically relevant networks (19, 20).
2. Introducing isotopically nonstationary measurements adds further complexity to experimental design. In addition to the design parameters that must be considered in the steady-state case, INST-MFA requires selection of sampling time points and metabolite concentration measurements. These new dimensions make the search for an optimal experiment design even more difficult and time-consuming. Several computational tools have been developed to efficiently traverse this design space, including parameterized sampling and a posteriori ranking of measurement time points (16, 21).

3. The labeling of intracellular metabolites in organisms with rapid metabolisms exhibits very short isotopic transients on the seconds time scale. Therefore, rapid sampling and quenching must be applied to obtain meaningful data. The field of metabolomics has witnessed considerable progress in this area, and some of these measurement techniques have already been successfully adapted for INST-MFA studies in *Escherichia coli* (1, 18).

Overall, INST-MFA holds great potential for future applications. INST-MFA experiments are already performed in a fraction of the time required for stationary MFA. If downstream sample processing and data analysis can be streamlined and automated, INST-MFA could soon become the basis for high-throughput MFA approaches (18, 22). It is also likely that INST-MFA will become the preferred approach for studies of plants, algae, and animal cell cultures, where labeling is slow and lack of long-term phenotypic stability can restrict the maximum duration of isotope tracer experiments. In this contribution, we present the necessary experimental techniques and computational procedures for performing INST-MFA, with the aim of making this approach accessible to a broader range of investigators within the metabolic engineering and metabolic physiology communities. We focus on those aspects of the analysis that are unique to INST-MFA and refer the reader to other literature on isotopomer measurement techniques and related methods that are common to both INST-MFA and steady-state MFA approaches. We also restrict ourselves to isotope labeling experiments performed on cultured cells, since this is the most common experimental system that has been used in INST-MFA studies to date.

2. Materials

2.1. ^{13}C Labeling Experiment

1. Cell culture at metabolic steady state (see Note 1).
2. Isotopically labeled substrates (see Note 2).
3. Syringes, valves, tubing, and associated equipment for introducing tracers and rapidly removing samples at precise time intervals.

2.2. Quenching and Metabolite Extraction

This protocol is appropriate for quenching and extraction of microbial cells based on a modified Folch extraction method (23). Refer to other references for quenching and extraction of plant cells (24) or mammalian cells (25).

1. Chloroform.
2. Methanol.

3. DI water.
4. Vortexer.
5. Benchtop centrifuge (capable of at least 5,000 rpm).
6. Centrifuge tubes (50 mL and 15 mL).

2.3. Extracellular Uptake and Excretion Flux Measurements

1. Cell culture at metabolic steady state (see Note 3).
2. Syringes, valves, tubing, and associated equipment for removing samples.
3. Analytical instruments (and associated reagents) for measuring extracellular metabolite concentrations, such as GC–MS, LC–MS, HPLC, biochemical analyzer, and microplate reader.

2.4. Mass Spectrometry Analysis

1. GC–MS and/or LC–MS.
2. Derivatization agents, vials, heating blocks, and nitrogen evaporator for GC–MS sample preparation (see Note 4).
3. Vials, columns, gases, buffers, solvents, and other consumables for GC–MS or LC–MS.

2.5. MS Data Processing

1. Computer equipped with either (1) freeware MS analysis software (see Note 5) or (2) commercial software for searching and integrating mass spectra.
2. Mass spectral library for compound verification, such as the NIST/EPA/NIH Mass Spectral Database (26), Golm Metabolome Database (27), FiehnLib (28), METLIN (29), HMDB (30), or MassBank (31).

2.6. Isotopically Nonstationary Metabolic Flux Analysis

1. Computer equipped with research code or publically available software capable of performing isotopically nonstationary metabolic flux analysis (INST-MFA), such as Isotopomer Network Compartmental Analysis (INCA; http://www.vanderbilt.edu/younglab), which runs through the computing environment of MATLAB.

3. Methods

3.1. ^{13}C Labeling Experiment

The ^{13}C labeling experiment should be initialized once a desired cell density has been attained, and the system is at metabolic steady state. A typical biomass sample size required for MS quantification is in the range of 1–10 mg of dry cell weight (9). Therefore, the volume and target cell density of the culture should be chosen so that repeated samples can be efficiently collected and processed without depleting the culture or significantly impacting its phenotypic state. It is suggested that cells be grown to the mid- to late

exponential growth phase before introducing the tracer to batch cultures, as this will provide for maximal cell densities and experimental repeatability. Alternatively, the experiment could be performed in a chemostat operating at an established steady state. Once the tracer has been introduced to the system, repeated samples should be withdrawn and rapidly quenched so that the labeling of intracellular metabolites can be accurately assessed at multiple time points during the transient labeling period.

1. *Introduce tracer to the system*. Labeled substrates can be dissolved in media and rapidly fed via syringe injection to a batch culture or by switching feed reservoirs to a chemostat culture. Autotrophic cultures that rely on gassed CO_2 can be connected to a $^{13}CO_2$-enriched gas feed. The introduction of tracer should not alter the chemical composition of the culture environment in a way that disturbs its metabolic steady state.
2. *Remove samples at multiple time points (~5–15) prior to reaching isotopic steady state*. Samples can be manually withdrawn using a syringe and needle at 20 s intervals, which is adequate for INST-MFA experiments with animal, plant, and slowly growing microbial cells. However, automated sampling techniques have been developed for applications to *E. coli* and other microbes that exhibit extremely fast isotopic transients in central metabolism (5). Samples should be collected more frequently near the beginning of the tracer experiment, as the isotopic labeling will be changing most rapidly during this initial time period. For example, Wiechert et al. (16) have recommended using an approach where the length of each time interval increases exponentially (e.g., 1, 2, 4, 8, and 16) following an initial period where uniformly spaced samples are collected at the maximum rate.

3.2. Quenching and Metabolite Extraction

1. After withdrawing each sample from the ^{13}C-labeled culture, initiate the quench by immediately spraying 1 volume of cell culture (containing 1–10 mg cell dry weight) into a 50 mL centrifuge tube containing 2 volumes of a 60/40 methanol/water solution at −40°C (see Note 6).
2. Separate cells from the quenching medium by centrifuging at 5,000 rpm for 5 min in a benchtop centrifuge precooled to the lowest temperature setting (e.g., −10°C). Aspirate the quench solution from the cell pellet.
3. Resuspend cells in 4 mL chloroform (−20°C).
4. Add 2 mL methanol (−20°C).
5. Vortex tubes for 30 min in cold room.
6. Add 1.5 mL ice-cold water.
7. Vortex tubes for additional 5 min.

8. Transfer to 15 mL centrifuge tubes.
9. Centrifuge at 5,000 rpm for 20 min at lowest temperature setting.
10. Collect aqueous (upper) phase in a new 15 mL tube or two microcentrifuge tubes.
11. Collect organic (lower) phase in a new 15 mL tube or two microcentrifuge tubes.
12. Add internal standards if quantification of metabolite concentrations is desired.
13. Evaporate all extracts to dryness using nitrogen at room temperature.
14. Store samples at −80°C.

3.3. Extracellular Uptake and Excretion Measurements

Extracellular uptake and excretion measurements are necessary to define the absolute scale of the intracellular fluxes and to constrain external fluxes that cross the system boundary. Regression analysis has been previously applied to determine metabolic fluxes from extracellular time courses of substrate depletion or product accumulation (32–35). However, if these measurements are unavailable, all fluxes can be normalized to a fixed "reference" flux (e.g., the net CO_2 uptake rate in autotrophic systems or the glucose uptake rate in heterotrophic systems). We have recently developed a program called ETA for performing the extracellular time-course analysis (see Note 7). It should be noted that these measurements typically require a separate unlabeled culture and a longer experimental time course than the ^{13}C labeling experiment.

3.4. Mass Spectrometry Analysis

The pathways of interest will dictate the types of metabolites and MS analysis to be performed. Generally, amino acids, organic acids, fatty acids, and sugars can be analyzed using GC–MS following chemical derivatization. Sugar phosphates and acyl-CoA molecules, on the other hand, are typically analyzed via LC–MS or LC–MS/MS, to avoid thermal degradation of these nonvolatile analytes. GC–MS analysis of a wide range of metabolites is most readily achieved by (1) methoximation to prevent keto-enol tautomerization followed by (2) conversion to trimethylsilyl (TMS) or *tert*-butyldimethylsilyl (TBMDS) derivatives (36). GC–MS analyses of derivatized amino acids, organic acids, and sugars are generally analyzed on nonpolar columns, while fatty acids are analyzed on polar columns. GC–MS analysis is typically performed in electron ionization (EI) mode to generate multiple fragment ions of the target analytes. LC–MS/MS analysis of sugar phosphates and acyl-CoA molecules can be accomplished using an ion-pairing gradient LC–MS/MS method with a nonpolar column and a solution of tributylamine + acetic acid as eluent A and methanol as eluent B (37). The acquisition of labeling and concentration data can be performed using negative electrospray ionization in multiple

reaction monitoring (MRM) mode. Initial suggestions for chromatographic parameters for GC–MS or LC–MS/MS are described by Roessner et al. (38) and Luo et al. (39), respectively. These parameters will typically need to be further optimized depending on the target analytes of interest and the complexity of the sample matrix.

3.5. MS Data Processing

Analysis of MS data requires (1) identification of chromatographic peaks and fragment ions associated with target analytes of interest, (2) integration of ion chromatograms over time to quantify relative abundance of specific isotope peaks, and (3) assessment of measurement standard errors. In many cases, it is also desirable to "correct" the raw mass isotopomer distributions (MIDs) to account for the presence of naturally occurring stable isotopes. Corrected mass isotopomer data provides a more intuitive picture of the labeling that is attributable to the introduction of a tracer compound and is generally the preferred method for presenting data from an isotope labeling experiment. However, some INST-MFA software, such as INCA, is capable of performing these corrections internally, and therefore, it is only necessary to input the raw, uncorrected MIDs.

1. *Identify the chromatographic peaks associated with the analytes of interest.* This is based on both the retention time (RT) and the MS fingerprint of the peak. Automated searching of mass spectral databases can facilitate the identification of compounds within complex mixtures. Furthermore, when pure standards of the target analytes are commercially available, these can be run separately or spiked into extract samples to confirm the identity of uncertain peaks.
2. *Identify ions to be used for mass isotopomer analysis and determine their molecular composition.* The best GC–EI-MS fragment ions are highly abundant ions with masses greater than 150 Da, since these are less likely to be contaminated by interfering fragment ions of similar mass. Determining the elemental composition of these ionic species is facilitated by references that list common fragmentation patterns and molecular rearrangements obtained for particular classes of compounds and derivatization groups (24, 40). The precursor ions formed in negative-ESI mode from LC–MS/MS analysis typically result from simple proton extraction. Since current application of LC–MS/MS to mass isotopomer analysis only makes use of product ions that are formed without breaking the carbon backbone of their precursor ions, the product ion spectra reflect the MIDs of the intact precursor ions when ^{13}C is used as tracer (41).

3. *Integrate the mass isotopomer peaks using either custom or commercial software*. In order to maximize the accuracy of mass isotopomer data, it is necessary to integrate each ion chromatogram over its full peak width and the exact same time window of integration. It is important for these parameters to be determined consistently for all mass isotopomers of a given fragment ion so that errors in the MID will not occur (42). This also involves integrating all single ion traces over all scans of the peak, including masses up to 3 Da heavier than the fully labeled fragment ion. For example, to quantify the MID of a fragment with monoisotopic mass 200 m/z and up to three-labeled carbons, extract and independently integrate the ion traces of 200, 201, 202,..., 206. Normalize the integrated areas such that the sum of all mass isotopomers for a given fragment ion is 1 (i.e., 100 mol %).
4. *Correct mass isotopomer distributions (MIDs) for natural isotope abundance (optional)*. The method of Fernandez et al. (43) can be applied to perform the correction.
5. *Calculate the mean and standard error of MIDs for each metabolite at each time point*. In order to perform statistical analysis of best-fit flux solutions, MFA software requires the user to input standard errors of each mass isotopomer measurement. Typically, the precision (i.e., repeatability) of these measurements is superior to their absolute accuracy (42). Inaccurate MIDs can occur due to interference from overlapping fragment ions or gas-phase proton exchanges that contaminate the mass spectrum of the target ions (44). Therefore, it is important to assess both precision and accuracy using standards of known isotope labeling. At minimum, it is necessary to run samples from naturally labeled cell extracts and compare the experimentally determined MIDs to theoretically predicted values. The approach of Fernandez et al. (43) can be used to predict MIDs of unlabeled samples based on reported values of elemental isotope abundance (45). A more thorough error assessment would also involve analyzing mixtures of labeled standards to quantify the uncertainty in measuring MIDs that differ from natural labeling (e.g., see Antoniewicz et al. (42)). In general, fragment ions used for MFA should be accurate to within 1.5 mol % (and preferably 0.8 mol %) of the predicted value (36).

3.6. Isotopically Nonstationary Metabolic Flux Analysis

A flow chart of a typical INST-MFA process is shown in Fig. 3. INST-MFA is concerned with solving an "inverse problem" where fluxes and pool sizes are estimated from measured labeling patterns and extracellular rates through the means of an iterative least-squares fitting procedure. At each iteration, a "forward problem" is solved where an isotopomer model is used to simulate labeling

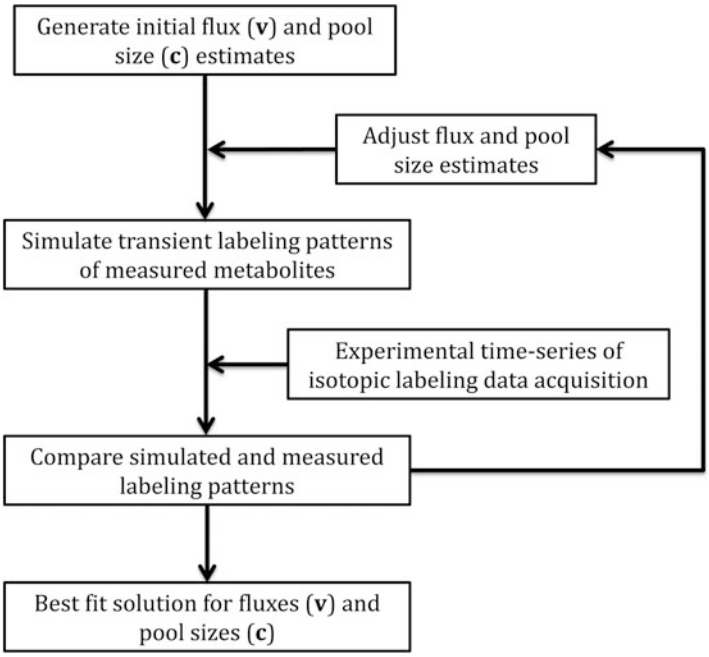

Fig. 3. Flowchart showing the overall schematic of ^{13}C INST-MFA. Following the labeling experiment and MS analysis of the measured metabolites, computational analysis of the dynamic changes in isotope labeling patterns can be used to estimate metabolic pathway fluxes and pool sizes. This involves solving an inverse problem whereby the vectors of flux (v) and pool size (c) parameters are iteratively adjusted until the mismatch between simulated and experimentally measured data sets is minimized.

measurements for a given metabolic network and a given set of parameter estimates. The discrepancy between the simulated and measured labeling patterns is then assessed, and the parameter estimates are updated to achieve an improving fit. Once convergence to the best-fit solution is obtained, the procedure terminates, and the optimal flux and pool size estimates are returned.

3.6.1. Build an Isotopomer Model for INST-MFA

In order to perform INST-MFA, it is necessary to reconstruct a metabolic network from biochemical literature and the annotated genome of the organism of interest. This network must prescribe both (1) the stoichiometry of all enzymatic reactions under consideration and (2) atom transitions for each reaction (see Note 8). Reactions must also be classified as either reversible or irreversible.

1. *Construct a stoichiometric model including all substrates, products, and intermediate metabolites.* When constructing a model, it is important to strive for parsimony in describing the available experimental measurements. The model must be sophisticated enough to reconcile all available experimental measurements while simultaneously avoiding unnecessary complexity and redundancy that leads to overfitting of

parameters. Fortunately, there are statistical tests to assess goodness-of-fit and to detect loss of precision due to overfitting (presented in Subheading 3.6.5). Overly sophisticated models can be reduced by (1) combining linear pathways into a single reaction, (2) combining isoenzymes or parallel pathways that catalyze identical conversions, and (3) omitting irrelevant pathways based on biological knowledge, such as repression of pathways under certain conditions (36). Additionally, if the cells are growing at a significant rate, all fluxes toward biomass production can be lumped into a single biosynthetic reaction that summarizes the withdrawal of all necessary growth precursors. Cofactors that contribute to energy balancing (e.g., ATP) or redox balancing (e.g., NADH or NADPH) are usually omitted from the model to ensure that these difficult-to-quantify balances do not unduly bias the resulting flux estimates (36).

Construction of a stoichiometric model can be further complicated by (1) compartmentalization of metabolites, (2) reaction reversibility, and (3) tracer dilution from unlabeled sources. First, as a result of subcellular compartmentalization in eukaryotes, the same biochemical reactions can occur simultaneously in different organelles, giving rise to multiple distinct metabolic pools that must be treated as separate nodes in the isotopomer model. Transport of metabolites between different compartments also needs to be defined in the model (e.g., exchange of pyruvate between the cytosol and mitochondria). Because each metabolite measurement obtained by MS analysis represents an aggregation of these different metabolic pools, pseudoreactions can be introduced into the model to represent the contribution from each compartment (see Note 9). However, this also introduces additional parameters into the model that must be determined from the isotopomer measurements. Second, reaction reversibility is another crucial consideration, since exchange fluxes (defined as the minimum of the forward and reverse reaction rates) affect metabolite labeling patterns in addition to net fluxes (defined as the difference between forward and reverse reaction rates). While all enzymes are reversible to some extent, many can be classified as practically unidirectional as a result of thermodynamic and kinetic considerations (e.g., pyruvate kinase in glycolysis). Third, enrichment of the tracer can also be diluted by unlabeled sources, such as CO_2 present in air, unlabeled carbon sources in complex culture media, or even breakdown of macromolecular biomass components. The inclusion of these unlabeled sources in the model can be critical to obtaining a statistically acceptable description of actual experimental data sets.

2. *Classify each metabolite as balanced or unbalanced.* Balanced metabolites are intermediate nodes for which the total incoming flux is constrained to balance the total outgoing flux. Unbalanced metabolites can refer to any carbon sources or sinks within the stoichiometric network, such as glucose or biomass, respectively. Additionally, unbalanced metabolites can also arise at intermediate nodes that exchange rapidly with the extracellular environment, as is often the case for CO_2. It is important to distinguish between balanced and unbalanced metabolites, since unbalanced metabolites do not impose stoichiometric constraints on the network and their labeling is typically considered to be fixed and externally specified.
3. *Specify the atom transitions for each reaction in the stoichiometric model.* It is necessary to include the atom transitions for each reaction present in the metabolic network so that the fate of each atom can be traced from substrate to product. Generally, the atom mapping for a particular enzyme is conserved between species and can be extracted from existing MFA models or articles found in biochemical literature. Furthermore, the model must account for the scrambling that occurs due to symmetric metabolites or chemically equivalent groups of atoms (20).
4. *Specify the tracer substrates and their positional ^{13}C labeling.* This information is necessary to define the labeled inputs to the isotopomer model.

3.6.2. Solve the Forward Problem to Simulate Labeling Measurements

In INST-MFA, the isotopomer balances are described by a system of ordinary differential equations, which is significantly more expensive to solve than the algebraic systems that describe steady-state labeling. Due to this additional difficulty, algorithms for solving the forward problem of INST-MFA need to be carefully designed so that computational expense does not become prohibitive. The most efficient approach involves first decomposing the isotopomer network into Elementary Metabolite Units (EMUs) (19, 20). By only solving for the isotopomer distributions of EMUs that contribute to the available measurements, this approach minimizes the number of ODEs that need to be integrated and thereby enables the forward problem to be solved thousands of times faster than previous methods. This, in turn, increases the efficiency of the inverse problem of INST-MFA because each iteration of the parameter estimation procedure can be completed in minimal time.

An EMU is defined as a distinct subset of a metabolite's atoms and can exist in a variety of mass states depending on its isotopic composition. In its lowest mass state, an EMU is referred to as M0, while an EMU that contains one additional atomic mass unit

(e.g., as a result of a ^{13}C atom in place of ^{12}C atom) is referred to as M1, with higher mass states described accordingly. An MID is a vector that contains the fractional abundance of each mass state of an EMU. To solve the forward problem of simulating metabolite labeling in INST-MFA, the isotopomer network is first systematically searched to enumerate all EMUs that contribute to measurable MS fragment ions. Then, these EMUs are grouped into mutually dependent blocks using a Dulmage–Mendelsohn decomposition (46, 47) (see Note 10). Therefore, by definition, all EMUs within a particular block have the same number of atoms and must be solved simultaneously and not sequentially.

The decoupled blocks can be arranged into a cascaded system of ODEs with the following form:

$$\mathbf{C}_n \cdot \frac{\mathrm{d}\mathbf{X}_n}{\mathrm{d}t} = \mathbf{A}_n \cdot \mathbf{X}_n + \mathbf{B}_n \cdot \mathbf{Y}_n \tag{1}$$

Level n of the cascade represents the network of EMUs within the nth block. The rows of the state matrix $\mathbf{X}_n$ correspond to MIDs of EMUs within the nth block. The input matrix $\mathbf{Y}_n$ is analogous but with rows that are MIDs of EMUs that are previously calculated inputs to the nth block (or MIDs of source EMUs that are unbalanced). The concentration matrix $\mathbf{C}_n$ is a diagonal matrix whose elements are pool sizes corresponding to EMUs represented in $\mathbf{X}_n$. The system matrices $\mathbf{A}_n$ and $\mathbf{B}_n$ describe the network as follows:

$$\mathbf{A}_n(i,j) = \begin{cases} -\text{sum of fluxes consuming, } i\text{th EMU in } \mathbf{X}_n & i = j \\ \text{flux to } i\text{th EMU in } \mathbf{X}_n \text{ from } j\text{th EMU in } \mathbf{X}_n & i \neq j \end{cases} \tag{2}$$

$$\mathbf{B}_n(i,j) = \{\text{flux to } i\text{th EMU in } \mathbf{X}_n \text{ from } j\text{th EMU in } \mathbf{Y}_n \tag{3}$$

1. *Simulate the time course of isotope labeling.* Given initial estimates of all fluxes and pool sizes, Eq. 1 can be constructed and then integrated. This can be accomplished using standard ODE numerical solvers or specialized algorithms that take advantage of the linear structure of this dynamical system, as described by Young et al. (19).
2. *Analyze the simulation results.* Solving the forward problem enables calculation of isotopomer distributions for each metabolite of interest, based on the initial flux and pool size estimates. The simulated MIDs can be plotted versus time and compared to the measured data. Fig. 4 shows an example of the labeling dynamics of several metabolites in an autotrophic system using ^{13}C-labeled bicarbonate as the tracer. The relative abundances of unlabeled mass isotopomers (M0) dropped at the start of the labeling period and were replaced by M1, M2, and higher mass isotopomers following the introduction of tracer. Additionally,

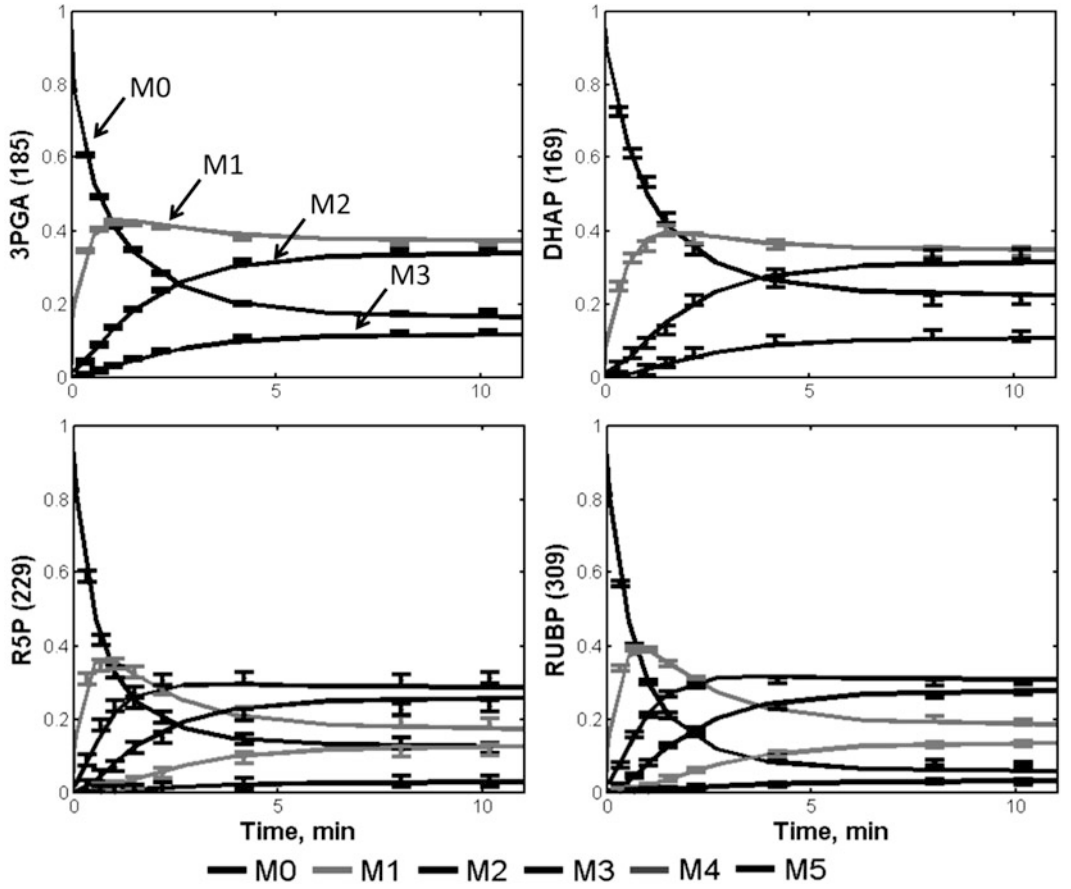

Fig. 4. Experimentally measured labeling trajectories of central metabolic intermediates (data points) and INST-MFA model fits (*solid lines*) from an autotrophic INST-MFA study. The *error bars* represent standard measurement errors. Ions shown are for 3-phosphoglycerate (3PGA), dihydroxyacetone phosphate (DHAP), ribose-5-phosphate (R5P), and ribulose-1,5-bisphosphate (RUBP). Nominal masses of M0 mass isotopomers are shown in parentheses (Adapted from Young et al. (10)).

it is also informative to plot the average enrichments of various MS fragment ions as shown in Fig. 5. The average ^{13}C enrichment is calculated using the following expression:

$$\frac{1}{N}\sum_{i=1}^{N} Mi \times i \tag{4}$$

where N is the number of carbon atoms in the metabolite and Mi is the fractional abundance of the ith mass isotopomer.

3.6.3. Sensitivity Calculation Estimation of both the unknown fluxes and pool sizes using INST-MFA is accomplished by finding a best-fit solution to the inverse problem. Efficient solution of this problem typically relies on optimization algorithms that choose the search direction based on the gradient of the least-squares objective function (see Eq. 6) with respect to all adjustable parameters. The most accurate and least

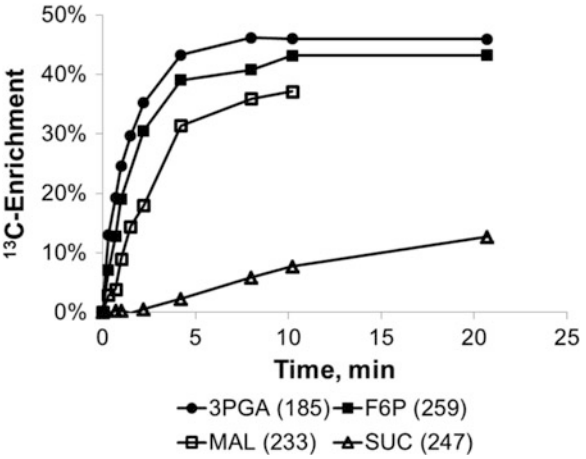

Fig. 5. Average ^{13}C enrichments of selected ion fragments from an autotrophic INST-MFA study. The labeling trajectory is shown for 3-phosphoglycerate (3PGA), fructose-6-phosphate (F6P), malate (MAL), and succinate (SUC) over the course of 10 min (Adapted from Young et al. (10)).

expensive way to obtain the required gradient information is to integrate a system of sensitivity equations whose solution describes how the calculated MIDs vary in response to changes in the model parameters. Implicit differentiation of Eq. 1 yields the following sensitivity equation:

$$\frac{\mathrm{d}}{\mathrm{d}t}\frac{\partial \mathbf{X}_n}{\partial \mathbf{p}} = \mathbf{C}_n^{-1}\cdot\mathbf{A}_n\cdot\frac{\partial \mathbf{X}_n}{\partial \mathbf{p}} + \frac{\partial\left(\mathbf{C}_n^{-1}\cdot\mathbf{A}_n\right)}{\partial \mathbf{p}}\cdot\mathbf{X}_n + \mathbf{C}_n^{-1}\cdot\mathbf{B}_n\cdot\frac{\partial \mathbf{Y}_n}{\partial \mathbf{p}} + \frac{\partial\left(\mathbf{C}_n^{-1}\cdot\mathbf{B}_n\right)}{\partial \mathbf{p}}\cdot\mathbf{Y}_n \tag{5}$$

where $\mathbf{p}$ is the vector of adjustable flux and pool size parameters. This system of equations can be solved in tandem with those of Eq. 1, and the time-dependent sensitivities can be used to evaluate the objective function gradient during each iteration of the INST-MFA inverse problem. Furthermore, if approximate values of the parameters are available prior to performing the labeling experiment, calculation of measurement sensitivities can provide useful information pertaining to parameter identifiability and experimental design.

3.6.4. Experimental Design

While solving the forward problem is an important step in the determination of fluxes using INST-MFA, it can also inform the experimental design. The precision with which a particular flux or pool size can be estimated, if at all, is solely determined by the sensitivity of the available measurements to the flux in question, which is a function of (1) the isotopic tracer applied, (2) the structure of the metabolic network, (3) the intracellular flux distribution, (4) the timing of the measurements, and (5) the

metabolites that are measured. Since (2) and (3) are not under the control of the experimenters, the key elements of experimental design entail choosing appropriate combinations of (1), (4), and (5) to identify the fluxes of interest. For the most part, the prevailing philosophy has been to measure as many metabolites as possible that are relevant to the pathways of interest. Therefore, the focus of experimental design has been on choosing the labeled substrate(s) and sampling strategy that will maximize the precision of flux estimates based on the available isotopic measurements. There is a wide literature on optimal design of ^{13}C labeling experiments, and the extension of these concepts to INST-MFA experiments has been presented by Wiechert and colleagues (16, 21).

3.6.5. Solving the Inverse Problem to Determine Flux and Pool Size Parameters

Fluxes and pool sizes are estimated by minimizing the difference between measured and simulated data according to the following equation (16, 20):

$$\min_{\mathbf{u},\mathbf{c}} \phi = [\mathbf{m}(\mathbf{u},\mathbf{c},\mathrm{t}) - \hat{\mathbf{m}}(t)]^T \cdot \sum_{m}^{-1} \cdot [\mathbf{m}(\mathbf{u},\mathbf{c},\mathrm{t}) - \hat{\mathbf{m}}(t)]$$
$$\text{s.t. } \mathbf{N}\cdot\mathbf{u} \geq 0,\ \ \mathbf{c} \geq 0$$

where ϕ is the objective function to be minimized, $\mathbf{u}$ is a vector of free fluxes, $\mathbf{c}$ is a vector of metabolite concentrations, t is time, $\mathbf{m}(\mathbf{u},\mathbf{c},t)$ is a vector of simulated measurements, $\hat{\mathbf{m}}(t)$ is a vector of observed measurements, $\mathbf{\Sigma_m}$ is the measurement covariance matrix, and $\mathbf{N}$ is the nullspace of the stoichiometric matrix. A reduced gradient method can be implemented to handle the linear constraints of this problem within a Levenberg–Marquardt nonlinear least-squares solver (48, 49). Alternatively, gradient-free optimization approaches have been applied by Noh et al. (16).

1. *Perform the flux estimation analysis by minimizing the difference between the measured and simulated measurements.* The flux estimation is performed by calculating the solution to Eq. 6. To ensure a global solution is obtained, it is advisable to repeat the parameter estimation from multiple initial guesses when using a gradient-based local optimization search. Alternatively, stochastic global optimization algorithms based on genetic programming or simulated annealing can be applied to ensure broad coverage of the parameter space.
2. *Assess the overall fit of the flux estimation.* Testing the goodness-of-fit will determine whether the optimal solution is statistically acceptable based on the minimized sum of squared errors (SSE). At convergence, the minimized variance-weighted SSE is a stochastic variable drawn from a chi-square distribution with n-p degrees of freedom (DOF), where n is the number of independent measurements and p is the number of estimated parameters. The SSE that is calculated should therefore be in the interval

$[\chi^2_{\frac{\alpha}{2}} \quad \chi^2_{1-\frac{\alpha}{2}}]$, where α is a chosen threshold value corresponding to the desired confidence level (e.g., 0.05 for 95 % confidence or 0.01 for 99 % confidence). The model fit is accepted when the SSE falls within the limits of the expected chi-square range (50). Additionally, the distribution of residuals should be assessed for normality. The standard deviation-weighted residuals should be normally distributed with a mean of zero and standard deviation of one. One approach that can be used to evaluate the hypothesis that the residuals are normally distributed is the Lilliefors test (51). Various plots can also be constructed to assess normality of the residuals.

3. *Assess the goodness-of-fit of each measurement.* In addition to checking the overall distribution of the residuals, it is often informative to plot the simulated and measured MIDs of each MS fragment ion. Furthermore, one should check the residuals between any measured extracellular fluxes and the estimates derived from INST-MFA. This provides a visual assessment of which measurements are mostly responsible for the lack of fit. If a poor fit is obtained, further investigation needs to be performed to identify the source of disagreement between experimental measurements and the isotopomer model. There are three possible causes for a poor fit that should be evaluated: (1) there are gross errors associated with the measurements, (2) there is an inappropriate weighting of the residuals, or (3) there is a mistake or omission in the metabolic reaction network. One should proceed by process of elimination to determine which of these is the root cause of a poor fit and then take corrective steps.
4. *Identify measurements that contribute significantly to the precision of estimated fluxes.* The fractional contribution of each measurement to the local variance of each flux can be calculated as described in Antoniewicz et al. (50). The higher the contribution value, the more important the measurement is for determining a particular flux. Fluxes that depend on only one measurement are very sensitive to errors in that one measurement. It is therefore desirable that more than one measurement significantly contributes to the estimation of each flux.

3.6.6. Calculate Parameter Uncertainties

Once an optimal solution has been obtained, nonlinear confidence intervals on the fitted parameters should be computed using robust, global methods instead of relying solely upon local standard errors. The local standard errors can be easily obtained from the parameter covariance matrix at the optimal solution; however, they do not accurately reflect changing sensitivities at points removed from the optimal solution. Furthermore, the calculation of the covariance matrix becomes ill conditioned when the Hessian of ϕ with respect to the fitted parameters is close to singular.

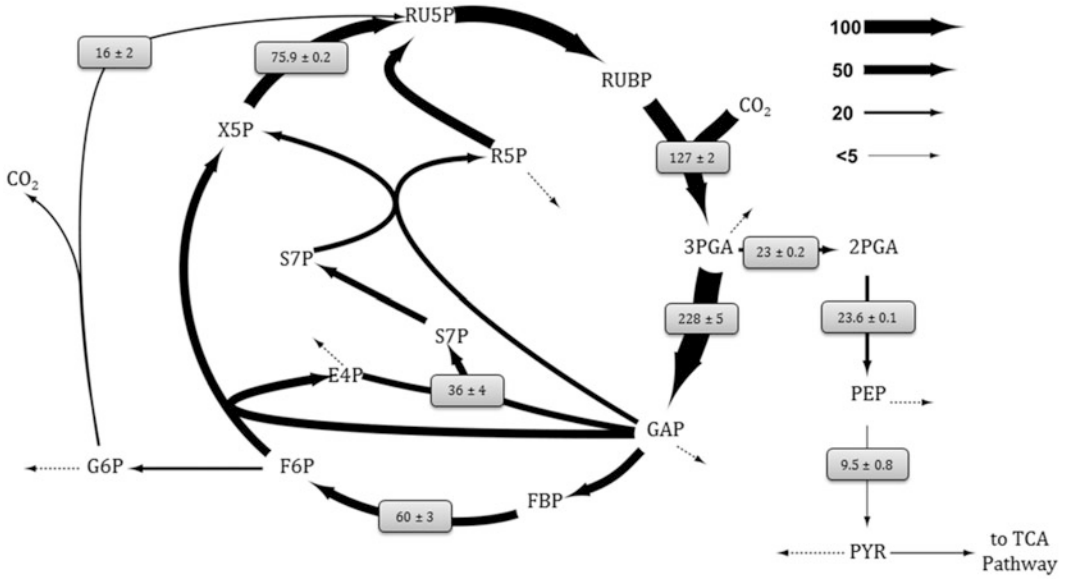

Fig. 6. Example of a flux map constructed for an INST-MFA study determined under photoautotrophic growth conditions. This flux map shows the estimated fluxes associated with glycolysis and the Calvin cycle for a *Synechocystis* INST-MFA study. Net fluxes are shown normalized to a net CO_2 uptake rate of 100. Values are represented as $M \pm SE$, where M is the median of the 95 % flux confidence interval and SE is the estimated standard error of M. Arrow thickness is scaled proportional to net flux. *Dotted arrows* indicate fluxes to biomass formation (Adapted from Young et al. (10)).

1. *Calculate the 95 % confidence intervals using either continuation methods or Monte Carlo analysis.* Parameter continuation can be performed to calculate accurate upper and lower bounds on the 95 % confidence interval for each flux or pool size parameter (50). This determines the sensitivity of the minimized SSE to varying a single parameter away from its optimal value while allowing the remaining parameters to adjust in order to minimize $\Delta\phi$. Large confidence intervals indicate that the flux cannot be estimated precisely. On the other hand, small confidence intervals indicate that the flux is well determined. Monte Carlo simulation can also be used to calculate the 95 % confidence intervals. This method is typically more expensive than the parameter continuation approach but is expected to yield similar results.

3.6.7. Report the Flux Values and Flux Uncertainties

Once an acceptable fit to the experimental measurements has been achieved and confidence intervals have been computed for all parameters, the results are best summarized visually in the form of a flux map. Fig. 6 shows an example of a flux map for the Calvin cycle and glycolytic pathway of *Synechocystis* sp. PCC6803 determined under photoautotrophic growth conditions using INST-MFA (10). Several software tools have been recently developed, which aid in the construction of these maps (see Note 11).

4. Notes

1. These cell cultures can be grown in flasks or bioreactors with working volumes ranging from 50 mL to 1 L, depending on the sampling volume and number of samples to be taken, as discussed in Subheading 3.6.4, "Experimental Design." Variables that should be controlled or monitored include temperature, pH, dissolved oxygen, and nutrient concentrations. Additionally, light intensity should be controlled for photoautotrophic cell cultures.
2. Until recently, most ^{13}C labeling experiments have been performed using labeled glucose tracers (e.g., [U-$^{13}C_6$]glucose, [1-^{13}C]glucose, [1,2-$^{13}C_2$]glucose, or mixtures thereof). However, INST-MFA studies of photoautotrophic systems, such as plants and cyanobacteria, by definition must rely on labeling solely from $^{13}CO_2$ or labeled bicarbonate. The choice of tracer(s) should be made to provide the maximum amount of information from the labeling dynamics while minimizing changes to the chemical composition of the medium; this is discussed further in Subheading 3.6.4, "Experimental Design."
3. The cell culture used for measuring extracellular uptake and excretion flux measurements should be different from the one used in the ^{13}C labeling experiment. This is due to the fact that this cell culture does not require isotope labeling, and the time course for this experiment will usually be longer than the ^{13}C labeling experiment.
4. Derivitization agents such as methoxyamine (MOX), trimethylsilane (TMS), or *tert*-butyl dimethylsilane (TBDMS) are typical for GC–MS analysis. The MOX reaction protects ketone and aldehyde functional groups and thereby prevents the formation of multiple TMS or TBDMS derivatives. This step is unnecessary if no ketone or aldehyde functional groups are present in the analytes of interest. TMS and TBDMS derivatives produce several characteristic fragment ions that facilitate identification (40). Huege et al. (24) provide a list of several GC–EI-MS ion fragments of TMS derivatives that have been used for isotopomer analysis. Ahn and Antoniewicz (52) provide a similar list for TBDMS derivatized metabolites.
5. Available GC–MS freeware include AMDIS (http://chemdata.nist.gov/mass-spc/amdis/) and Wsearch32 (http://www.wsearch.com.au/wsearch32/wsearch32.htm). Two popular freeware programs for LC–MS/MS data analysis are MZmine and XCMS, the latter of which runs in the R statistical programming environment. Both programs require the user to convert raw data files into a nonproprietary format such as

mzXML, NetCDF, or mzData. Conversion to mzXML format can be accomplished using one of several instrument-specific software tools developed and maintained by the Seattle Proteome Center (http://tools.proteomecenter.org/software.php).

6. A −40°C bath can be achieved by creating a slurry of 4.5 M calcium chloride chilled in a −80°C freezer for 3–4 h prior to the start of the quench.
7. Extracellular Timecourse Analysis (ETA) is a software package that has been coded in MATLAB (http://mfa.vueinnovations.com). It can be used to estimate the specific growth rate as well as the cell-specific uptake and excretion rates of extracellular metabolites based upon time-course concentration measurements.
8. Networks used for heterotrophic MFA typically include glycolysis, pentose phosphate pathway, amino acid metabolism, TCA cycle, and various amphibolic pathways that interact with the TCA cycle. This backbone of central metabolic pathways may be further augmented by additional reactions of interest. Some helpful online databases include KEGG (Kyoto Encyclopedia of Genes and Genomes; http://www.genome.jp/kegg/), BioCyc (http://biocyc.org/), metaTIGER http://www.bioinformatics.leeds.ac.uk/metatiger/), ENZYME (http://enzyme.expasy.org/), and BRENDA (http://www.brenda-enzymes.info/).
9. One way to model pseudoreactions of compartmental mixing in INCA is as follows:

$$0^{*}\text{G6P.plastid (abcdef)} \rightarrow \text{G6P.pseudo (abcdef)}$$

$$0^{*}\text{G6P.cytosol (abcdef)} \rightarrow \text{G6P.pseudo (abcdef)}$$

$$\text{G6P.pseudo} \rightarrow \text{Sink (flux fixed to 100)}$$

These equations signify glucose-6-phosphate (G6P) coming from two different compartments, the plastid and cytosol. The letters in parentheses are the carbon atoms associated with G6P. The "0" in front of the first two reactions indicates that no carbon is actually withdrawn from the network, even though the carbon labeling is preserved in the G6P pseudometabolite (i.e., this essentially creates the G6P pseudometabolite without siphoning carbon away from the "real" metabolic network). The third reaction has a fixed flux set to an arbitrary value of 100 so that the fluxes estimated for the first two reactions represent the relative percentage contributions from the two compartments. More pseudoreactions may be added as more compartments are included in complex networks.

10. Blocks are defined by sets of EMUs whose MIDs are mutually dependent within the context of the EMU reaction network.

The EMUs are arranged into blocks where the EMU reaction network is regarded as a directed graph, where the nodes represent EMUs and edges represent EMU reactions. An $N \times N$ adjacency matrix is constructed for the directed graph, where N is the total number of EMUs. A nonzero entry $a(i, j)$ of the adjacency matrix indicates the dependence of the ith EMU's MID on the jth EMU's MID. A Dulmage–Mendelsohn decomposition is performed on the adjacency matrix, returning an upper block triangular matrix from which the diagonal blocks are extracted. Blocks can be arranged so that each is a self-contained subproblem that depends on the outputs of previously solved blocks, creating a cascaded system.

11. Several tools have been recently developed for flux visualization in the context of metabolic networks, such as FluxMap (53), FluxViz (54), faBINA (55), Omix (56), BioCyc Omics Viewer (57), Reactome Skypainter (58), Pathway Projector (59), MetaFluxNet (60), and OptFlux (61).

Acknowledgements

This work was supported by NSF EF-1219603. LJJ was supported by a GAANN fellowship from the US Department of Education under grant number P200A090323.

References

1. Wiechert W (2001) 13C metabolic flux analysis. Metab Eng 3:195–206
2. Sauer U (2006) Metabolic networks in motion: 13C-based flux analysis. Mol Syst Biol 2:62
3. Antoniewicz MR, Kraynie DF, Laffend LA et al (2007) Metabolic flux analysis in a nonstationary system: fed-batch fermentation of a high yielding strain of *E. coli* producing 1,3-propanediol. Metab Eng 9:277–292
4. Noguchi Y, Young JD, Aleman JO et al (2009) Effect of anaplerotic fluxes and amino acid availability on hepatic lipoapoptosis. J Biol Chem 284:33425–33436
5. Nöh K, Grönke K, Luo B et al (2007) Metabolic flux analysis at ultra short time scale: isotopically non-stationary 13C labeling experiments. J Biotechnol 129:249–267
6. Leighty RW, Antoniewicz MR (2011) Dynamic metabolic flux analysis (DMFA): a framework for determining fluxes at metabolic non-steady state. Metab Eng 13:745–755
7. Lequeux G, Beauprez J, Maertens J et al (2010) Dynamic metabolic flux analysis demonstrated on cultures where the limiting substrate is changed from carbon to nitrogen and vice versa. J Biomed Biotechnol 2010:1–19
8. Wahl SA, Nöh K, Wiechert W (2008) 13C labeling experiments at metabolic nonstationary conditions: an exploratory study. BMC Bioinforma 9:152
9. Shastri AA, Morgan JA (2007) A transient isotopic labeling methodology for 13C metabolic flux analysis of photoautotrophic microorganisms. Phytochemistry 68:2302–2312
10. Young JD, Shastri AA, Stephanopoulos G et al (2011) Mapping photoautotrophic metabolism with isotopically nonstationary (13)C flux analysis. Metab Eng 13:656–665
11. Zhao Z, Kuijvenhoven K, Ras C et al (2008) Isotopic non-stationary 13C gluconate tracer method for accurate determination of the pentose phosphate pathway split-ratio in *Penicillium chrysogenum*. Metab Eng 10:178–186

12. Maier K, Hofmann U, Bauer A et al (2009) Quantification of statin effects on hepatic cholesterol synthesis by transient (13)C-flux analysis. Metab Eng 11:292–309
13. Maier K, Hofmann U, Reuss M et al (2008) Identification of metabolic fluxes in hepatic cells from transient 13C-labeling experiments: part II. Flux estimation. Biotechnol Bioeng 100:355–370
14. Munger J, Bennett BD, Parikh A et al (2008) Systems-level metabolic flux profiling identifies fatty acid synthesis as a target for antiviral therapy. Nat Biotechnol 26:1179–1186
15. Iwatani S, Yamada Y, Usuda Y (2008) Metabolic flux analysis in biotechnology processes. Biotechnol Lett 30:791–799
16. Nöh K, Wahl A, Wiechert W (2006) Computational tools for isotopically instationary 13C labeling experiments under metabolic steady state conditions. Metab Eng 8:554–577
17. Wiechert W, Nöh K (2005) From stationary to instationary metabolic flux analysis. Adv Biochem Eng Biotechnol 92:145–172
18. Schaub J, Mauch K, Reuss M (2008) Metabolic flux analysis in *Escherichia coli* by integrating isotopic dynamic and isotopic stationary 13C labeling data. Biotechnol Bioeng 99:1170–1185
19. Young JD, Walther JL, Antoniewicz MR et al (2008) An elementary metabolite unit (EMU) based method of isotopically nonstationary flux analysis. Biotechnol Bioeng 99:686–699
20. Antoniewicz MR, Kelleher JK, Stephanopoulos G (2007) Elementary metabolite units (EMU): a novel framework for modeling isotopic distributions. Metab Eng 9:68–86
21. Noh K, Wiechert W (2006) Experimental design principles for isotopically instationary C labeling experiments. Biotechnol Bioeng 94:234–251
22. Sauer U (2004) High-throughput phenomics: experimental methods for mapping fluxomes. Curr Opin Biotechnol 15:58–63
23. Folch J, Lees M, Stanley GH (1957) A simple method for the isolation and purification of total lipides from animal tissues. J Biol Chem 226:497–509
24. Huege J, Sulpice R, Gibon Y et al (2007) GC-EI-TOF-MS analysis of in vivo carbon-partitioning into soluble metabolite pools of higher plants by monitoring isotope dilution after $13CO_2$ labelling. Phytochemistry 68:2258–2272
25. Yoo H, Antoniewicz MR, Stephanopoulos G et al (2008) Quantifying reductive carboxylation flux of glutamine to lipid in a brown adipocyte cell line. J Biol Chem 283:20621–20627
26. Ausloos P, Clifton CL, Lias SG et al (1999) The critical evaluation of a comprehensive mass spectral library. J Am Soc Mass Spectrom 10:287–299
27. Kopka J, Schauer N, Krueger S et al (2005) GMD@CSB.DB: the Golm Metabolome Database. Bioinformatics 21:1635–1638
28. Kind T, Wohlgemuth G, Lee DY et al (2009) FiehnLib: mass spectral and retention index libraries for metabolomics based on quadrupole and time-of-flight gas chromatography/mass spectrometry. Anal Chem 81:10038–10048
29. Smith CA, O'Maille G, Want EJ et al (2005) METLIN: a metabolite mass spectral database. Ther Drug Monit 27:747–751
30. Wishart DS, Tzur D, Knox C et al (2007) HMDB: the Human Metabolome Database. Nucleic Acids Res 35:D521–D526
31. Horai H, Arita M, Kanaya S et al (2010) MassBank: a public repository for sharing mass spectral data for life sciences. J Mass Spectrom 45:703–714
32. Glacken MW, Adema E, Sinskey AJ (1988) Mathematical descriptions of hybridoma culture kinetics: I. Initial metabolic rates. Biotechnol Bioeng 32:491–506
33. Goudar CT (2012) Computer programs for modeling mammalian cell batch and fed-batch cultures using logistic equations. Cytotechnology 64(4):465–475
34. Kim J-w, Tchernyshyov I, Semenza GL et al (2006) HIF-1-mediated expression of pyruvate dehydrogenase kinase: a metabolic switch required for cellular adaptation to hypoxia. Cell Metab 3:177–185
35. Zupke C, Sinskey AJ, Stephanopoulos G (1995) Intracellular flux analysis applied to the effect of dissolved oxygen on hybridomas. Appl Microbiol Biotechnol 44:27–36
36. Zamboni N, Fendt S-M, Rühl M et al (2009) (13)C-based metabolic flux analysis. Nat Protoc 4:878–892
37. Oldiges M, Kunze M, Degenring D et al (2004) Stimulation, monitoring, and analysis of pathway dynamics by metabolic profiling in the aromatic amino acid pathway. Biotechnol Prog 20:1623–1633
38. Roessner U, Wagner C, Kopka J et al (2000) Technical advance: simultaneous analysis of metabolites in potato tuber by gas chromatography–mass spectrometry. Plant J 23:131–142
39. Luo B, Groenke K, Takors R et al (2007) Simultaneous determination of multiple intracellular metabolites in glycolysis, pentose phosphate pathway and tricarboxylic acid cycle by

liquid chromatography-mass spectrometry. J Chromatogr A 1147:153–164
40. Kitson FG, Larsen BS, McEwen CN (1996) Gas chromatography and mass spectrometry: a practical guide. Academic, San Diego
41. Kiefer P, Nicolas C, Letisse F et al (2007) Determination of carbon labeling distribution of intracellular metabolites from single fragment ions by ion chromatography tandem mass spectrometry. Anal Biochem 360:182–188
42. Antoniewicz MR, Kelleher JK, Stephanopoulos G (2007) Accurate assessment of amino acid mass isotopomer distributions for metabolic flux analysis. Anal Chem 79:7554–7559
43. Fernandez CA, Des Rosiers C, Previs SF et al (1996) Correction of 13C mass isotopomer distributions for natural stable isotope abundance. J Mass Spectrom 31:255–262
44. Allen DK, Shachar-Hill Y, Ohlrogge JB (2007) Compartment-specific labeling information in 13C metabolic flux analysis of plants. Phytochemistry 68:2197–2210
45. Coplen TB, Bohlke JK, De Bievre P et al (2002) Isotope-abundance variations of selected elements: (IUPAC technical report). Pure Appl Chem 74:1987–2017
46. Dulmage AL, Mendelsohn NS (1958) Coverings of bipartite graphs. Canad J Math 10:517–534
47. Pothen A, Fan CJ (1990) Computing the block triangular form of a sparse matrix. ACM Trans Math Softw 16:303–324
48. Gill PE, Murray W, Wright MH (1981) Practical optimization. Academic, London
49. Madsen K, Nielsen HB, Tigleff O (2004). Methods for non-linear least squares problems. http://www2.imm.dtu.dk/pubdb/views/publication_details.php?id=3215.
50. Antoniewicz MR, Kelleher JK, Stephanopoulos G (2006) Determination of confidence intervals of metabolic fluxes estimated from stable isotope measurements. Metab Eng 8:324–337
51. Conover WJ (1999) Practical nonparametric statistics. Wiley, New York
52. Ahn WS, Antoniewicz MR (2011) Metabolic flux analysis of CHO cells at growth and non-growth phases using isotopic tracers and mass spectrometry. Metab Eng 13:598–609
53. Rohn H, Hartmann A, Junker A et al (2012) FluxMap: a VANTED Add-on for the visual exploration of flux distributions in biological networks. BMC Syst Biol 6:33
54. König M, Holzhütter H-G (2010) Fluxviz—cytoscape plug-in for visualization of flux distributions in networks. Genome informatics International conference on genome informatics 24:96–103
55. Hoppe A, Hoffmann S, Gerasch A et al (2011) FASIMU: flexible software for flux-balance computation series in large metabolic networks. BMC Bioinformatics 12:28
56. Droste P, Miebach S, Niedenführ S et al (2011) Visualizing multi-omics data in metabolic networks with the software Omix: a case study. Biosystems 105:154–161
57. Paley SM, Karp PD (2006) The pathway tools cellular overview diagram and omics viewer. Nucleic Acids Res 34:3771–3778
58. Matthews L, Gopinath G, Gillespie M et al (2009) Reactome knowledgebase of human biological pathways and processes. Nucleic Acids Res 37:D619–D622
59. Kono N, Arakawa K, Ogawa R et al (2009) Pathway projector: web-based zoomable pathway browser using KEGG atlas and Google Maps API. PLoS One 4:e7710
60. Lee SY, Lee D-Y, Hong SH et al (2003) MetaFluxNet, a program package for metabolic pathway construction and analysis, and its use in large-scale metabolic flux analysis of *Escherichia coli*. Genome informatics International conference on genome informatics 14:23–33
61. Rocha I, Maia P, Evangelista P et al (2010) OptFlux: an open-source software platform for in silico metabolic engineering. BMC Syst Biol 4:45